STRUCTURAL AND MAGNETIC PROPERTIES OF COBALT-CADMIUM FERRITES

[1]*T.R.K.Pydiraju, [2]P.Apparao, [3]K.H.Rao

[1]Asst. Professor, [2]Asst. Professor, [3] Professor

[1,2]Basic sciences & Humanities Department, [3]Physics Department

[1,2] Dadi Institute of Engineering & Technology, Anakapalle, India, [3]RGUKT, Nuzuvidu, India

Abstract : $Co_{1-x}Cd_xFe_2O_4$ (x=0.07 to 0.42) samples synthesized by sol-gel method. X-ray diffraction patterns have shown single phase spinel structure in all the samples. A reasonable cation distribution has been proposed using experimental data collected from Vibration Sample Magnetometer, X-ray diffraction. A high value of specific saturation magnetization, 104.54emu/gm has been obtained for x=0.07. The grain size of these samples has been observed to be in the range of 436 nm – 552nm as seen from FE-SEM pictures. Room temperature hysteresis loops establish the existence of A-B exchange interaction in all the samples.

IndexTerms* - *lattice constant, saturation magnetization, grain size.

I. INTRODUCTION

Ferrites consists of joint properties of magnetic materials and insulators [1]. The important structural, electrical and magnetic properties of these spinels, responsible for their applications in various fields, are found to depend on the magnetic interaction and the distribution of cations among the two sublattices, tetrahedral (A) and octahedral (B) sites. Among various spinel ferrites, cobalt ferrite based composites have received interest because of their high magnetostriction, high sensitivity of magnetic induction to applied stress, chemical stability and low-cost [2-6]. $CoFe_2O_4$ possesses a partially inverse spinel structure [7] and the degree of inversion depends upon heat treatment, synthesis method and substitution of metal ions [8]. The partial replacement of cobalt with diamagnetic ions (e.g. zinc or cadmium) may weaken the exchange interactions between A- and B-sites and result in decrease of the magnetic hyperfine field as well as the Curie temperature [9].

Very few studies have been reported on mixed Co-Cd systems. Non-collinear spin structure has been observed by Ghani and Sattar [10] in $Co_{1-x}Cd_xFe_2O_4$ from high field magnetization study in the temperature range 4.2 to 300K. For low concentration of Cd^{2+} ($x \leq 0.25$) Neel's two-sublattice model was observed by Vasambekar et al. [8], where for higher concentrations canted spin model existed for which they calculated Yafet-Kittel (Y-K) angles. Nikumbh et al. [11] prepared $Cd_{1-x}Co_xFe_2O_4$ (X = 0, 0.2, 0.4, 0.6, 0.8 and 1) by the tartrate coprecipitation technique and attempted to find the effect of cadmium ferrite spinel formation and the role of cobalt content on its structural, magnetic and electrical properties. However, there is no reported work in the literature on the FE-SEM and FTIR studies of Co–Cd ferrites synthesized by the sol-gel method of mixed metal nitrates with PVA as chelating agent. The aim of the present study is to understand the effect of cadmium ions on structural and magnetic properties of cobalt ferrite spinel by X-ray diffraction (XRD), FESEM, FTIR and VSM measurements at room temperature.

II. PREPARATION OF SAMPLES

Sol-gel method has been selected based on the previous reports especially in the field of ferrites, as it provides excellent control over purity and composition as well as on the size of the materials. Cadmium doped $CoFe_2O_4$ ferrites have been synthesized by sol-gel method as reported by KS Rao et al [12]. Analytical grade iron nitrate $Fe(NO_3)_3.9H_2O$ Cadmium nitrate $Cd(NO_3)_2.4H_2O$ and Cobalt nitrate $Co(NO_3)_2.6H_2O$ were weighed according to the required stoichiometric proportions and dissolved in a minimum amount of de-ionized water. The molar ratio of total metal ions to vinyl alcohol monomer units of PVA is maintained at 1:3. Annealing is done at 400ºC for dried powders and sintered at 1050ºC for 1 hour with a slow heating rate of 5ºC/minute in a programmable muffle furnace.

III. EXPERIMENTAL DETAILS

The XRD measurements have been carried out using Bruker D8 Advance X-ray diffractometer. The morphology of grains has been investigated by field-emission scanning electronic microscopy (FE-SEM). The infrared patterns were recorded using infrared spectrometer Thermo Nicolet IR200 in the range 370 cm^{-1} - 4000 cm^{-1}. The samples were prepared in the form of pellets in the KBr medium. Magnetic hysteresis loops have been recorded using Vibrating Sample Magnetometer with the maximum applied field of 5T to 7T at room temperature.

IV. RESULTS AND DISCUSSIONS

4.1. XRD studies: The X - ray diffraction patterns of all the compositions indicate the formation of a single spinel phase structure (Fig. 1). The experimentally observed d - spacing values and relative intensities were compared with those reported in literature [13]. The lattice parameter for each composition was then calculated using Nelson- Riley function [14] and listed in Table:1. The variation of lattice parameter "a" as a function of cadmium addition *x* in $Co_{1-x}Cd_xFe_2O_4$ is represented in Fig. 2.

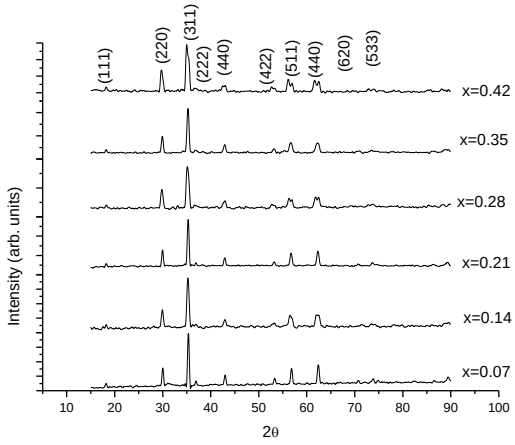

Figure 1: Variation of Intensity with 2θ for all samples with increasing Cd.

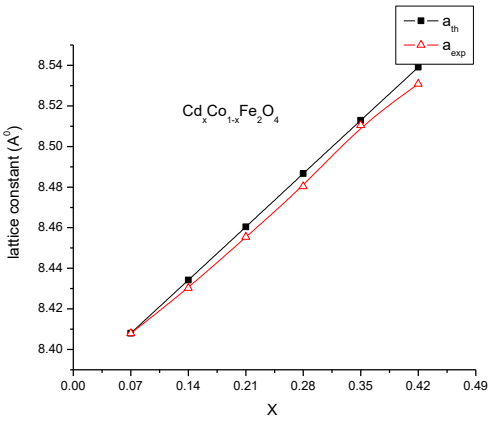

Figure:2 shows variation of lattice constant with Cd. Conc.

4.2. FESEM-EDS studies: FE-SEM images of the $Co_{1-x}Cd_xFe_2O_4$ ferrites are shown below. The above pictures show grains with octahedron shapes with wide distribution in grain sizes. From FESEM pictures it is clearly visible that no secondary phases are present at grain boundaries. Sharp edges and shapes of grains confirm the crystallinity of the synthesized samples. This is in accordance with XRD results, and confirms the purity of the samples.

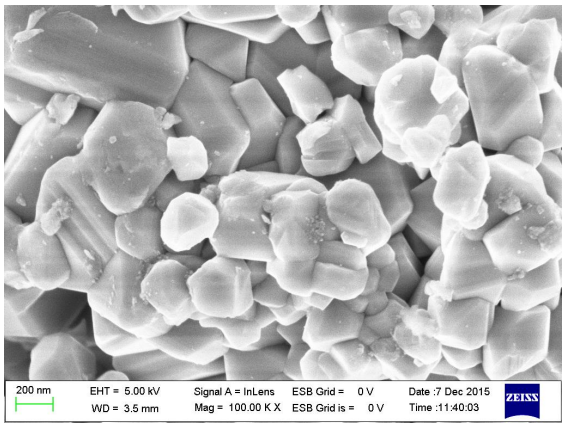

X= 0.07

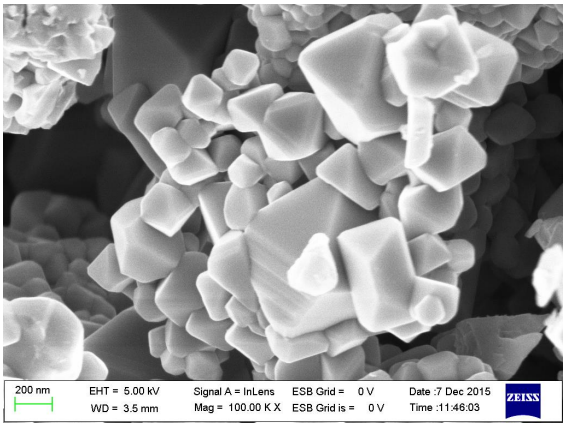

X=0.14

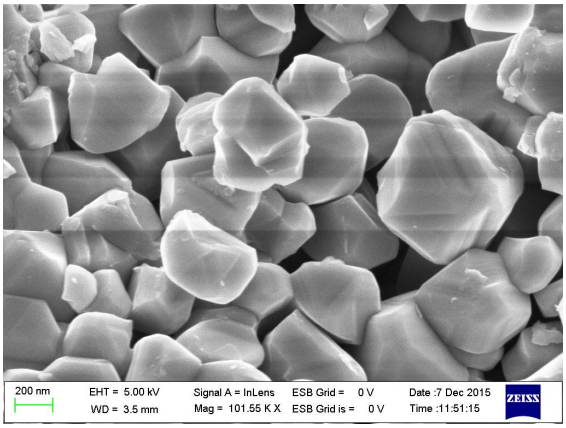

X= 0.21

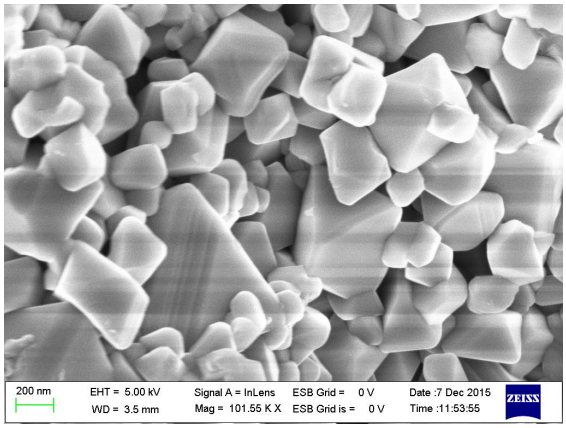

X=0.28

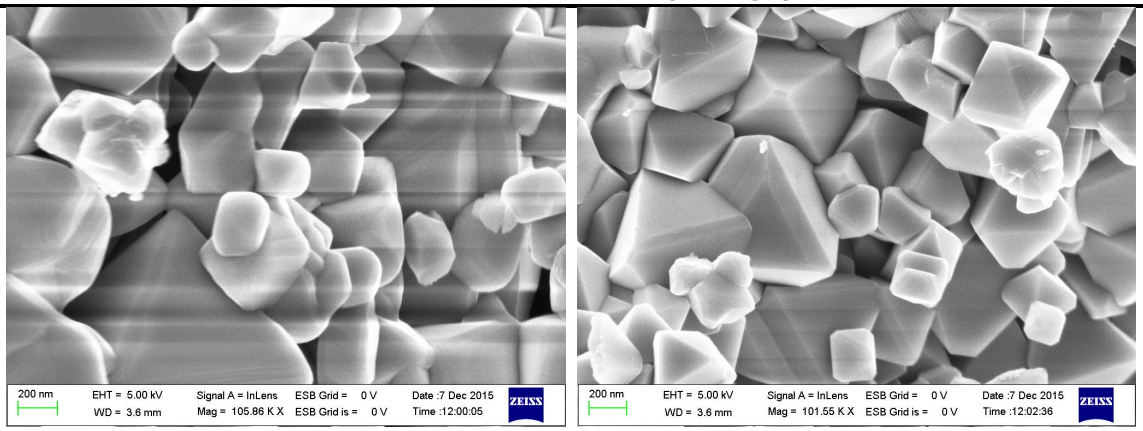

X= 0.35 X=0.42

Figure 3: Typical FE-SEM images of the $Co_{1-x}Cd_xFe_2O_4$ferrites with increasing Cd Conc.(x)

4.3. Grain Size: Grain size is determined using line intercept method and is found to be in the range of 436nm to 552nm for present samples. Figure 4 shows the variation of Grain-size with increasing cadmium concentration. The nonlinear behavior in variation of grain size shows that the dopant cadmium is playing a major role in controlling the morphology.

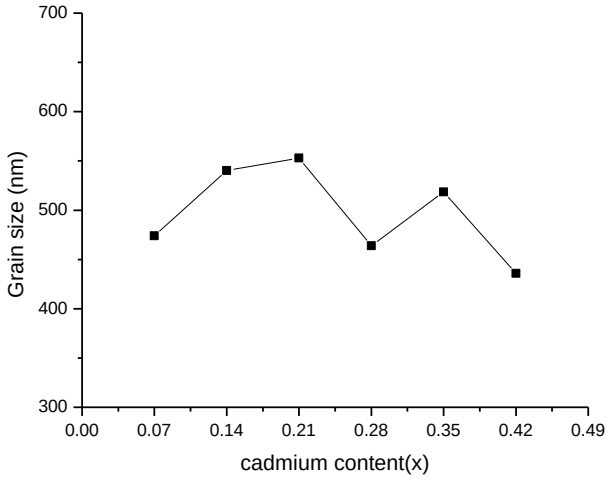

Figure 4: Variation of Grain-size with increasing Cd Conc.(x)

4.4. Infrared spectral studies: The spectra of all the ferrites have been used to locate the band positions are tabulated in Table 1. It is observed that the spectral bands are broadening more and more for higher contents of cadmium. Such broadening is commonly observed in inverse spinel ferrites. The broadening is due to the statistical distribution of iron ions at A-and B-sites. The band positions for these compounds $Co_{1-x}Cd_xFe_2O_4$ are in good agreement with those reported earlier [11,18,19] and shown in figure:5. An infrared spectrum of the present samples reveal that the absorption band around 600 cm^{-1} does not show any splitting or shoulders and the possibility of Fe^{+2} at the A - site is ruled out. There is evidence of a weak shoulder or splitting the absorption band around 400 cm^{-1} suggesting the possible presence of Fe^{+2} at the B-site, but this is not clearly established. The results are in general agreement with literature [19]. Tarte and Coworkers [21] have observed that in ferrites, both the absorption bands depend on the nature of octahedral cations and do not significantly depend on the tetrahedral ions. However, Waldron [22] and Hafner [23] attributed the band ν_1 at around 600 cm^{-1} to the intrinsic vibrations of tetrahedral metal oxygen complexes and the band ν_2 at around 400cm^{-1} to the intrinsic vibrations of octahedral complexes. The difference in band positions is because of the difference in the $Fe^{+3} - O^{-2}$ distances for the octahedral and tetrahedral complexes. The vibrational frequencies depend on cation mass, cation-oxygen distance and the bonding force. In an inverse spinel ($CoFe_2O_4$), the octahedral site is occupied by Fe^{+3} and the divalent ion Co^{+2}. Due to charge imbalance the oxygen ion is likely to shift towards the Fe^{+3} ion making the force constant between Fe^{+3} and O^{-2} more. Hence we expect a decrease in bond stretching mode, frequencies as we go from inverse to normal spinel. This is supported by our results on $Co_{1-x}Cd_xFe_2O_4$ in which we find that ν_1 decreases as x is increased, and ν_2 do not change with the type of spinel structure as shown in figure:6.

The force constants K_t (tetrahedral site) and K_o (octahedral site) for Fe-O have been obtained from the IR absorption data using the method of Waldron [22] and here $m = 2.061\times10^{-23} gm$ is reduced mass of Fe^{+3} and O^{-2}. The bond lengths d_{AX} and d_{BX} have been computed using the formula [24]. The variations of K_t and K_o with d_{AX} and d_{BX} are shown in figure:7.

$$K_t = 4\pi^2\nu_1^2c^2m$$

$$K_o = 4\pi^2\nu_2^2c^2m$$

$$d_{AX} = \sqrt{3}\, a_{th}\left(U - \frac{1}{4}\right)$$

$$d_{BX} = a_{th}\left(\frac{5}{8} - U\right)$$

A-site ionic radius has been observed to increase whereas that of B-site reduced with increasing cadmium content (table:1). Based on the earlier reports we assume that substituting cadmium ions in place of cobalt ions transfers Fe^{3+} ions from the tetrahedral site to octahedral site. Since Cd^{2+} ions have larger ionic radius compared to Fe^{3+} ions, and Cd^{2+} ions occupy A-sites, this leads to increase in A-site radius as well as lattice constant.

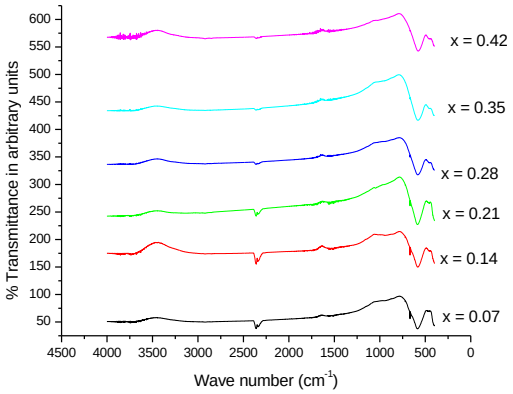

Fig 5: FTIR spectra with Cd Conc. (x).

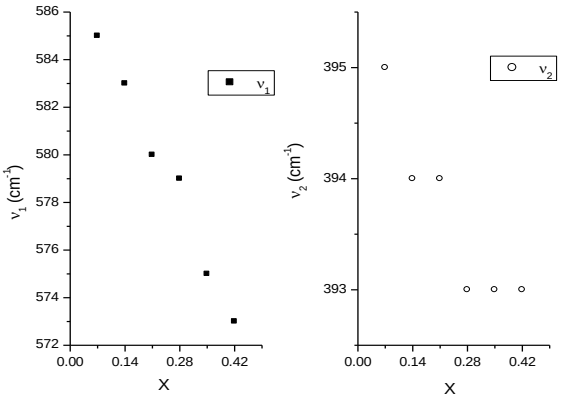

Fig 6: Variation of band wavenumbers ν_1& ν_2 at A and B-site with Cd

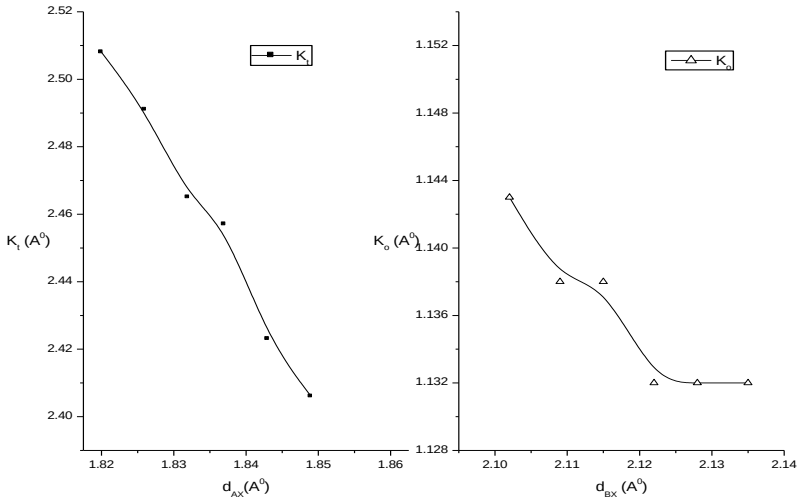

Figure 7: Variation of force constants (K) with bond lenghts at A-site & B-site.

The bond lengths d_{AX} and d_{BX} have been computed using the formula [18].

$$d_{AX} = \sqrt{3}\, a_{th}\left(U - \frac{1}{4}\right) \text{ and } d_{BX} = a_{th}\left(\frac{5}{8} - U\right)$$

Srivastava et al.[19] stated that the bond stretching for tetrahedral site would lead to higher force constants than that for octahedral site. Our results are consistent with their conclusion.The agreement in lattice constant and bond angles between experimental and those calculated based on predicted cation distribution clearly shows that the given cation distribution is correct. The same will be utilized in understanding the variations in magnetic properties.

4.5. Magnetic studies: Magnetic hysteresis curves for the system of $Cd_xCo_{1-x}Fe_2O_4$ which were obtained by Vibrating sample magnetometer at a field intensity of 5T to 7T as shown in figure:8. The magnetic parameters like the coercive field(H_c), saturation magnetization(M_s), ratio of remanence to saturation magnetization (M_R/M_s), magnetic moment(n_B) and Y-K angles(α_{YK}) values are listed in table:2. Magnetic moment, H_c, M_s and M_R/M_s have been observed to decreased with increasing Cd^{2+} content. These variations can be understood from the strong preference of Cd^{+2} and Co^{+2} ions to A and B sites respectively [11]. Cation distribution

has been proposed as $(Cd_xCo_y\ Fe_{1-x-y})_A[Co_{1-x-y}\ Fe_{1+x+y}]_B$ and magnetic moment can be calculated using [3(1-x-y)+5(1+x+y)]-[3y+5(1-x-y)] by considering the magnetic moment of Co^{+2} ions as $3\mu_B$ and that of Fe^{+3} ions as $5\mu_B$.

The substitution of diamagnetic Cd^{+2} ions at A-site may cause some Fe^{+3} ions to migrate to B-sites. Due to dilution of A-sites by Cd^{2+} ions, magnetic moment at this site decreases and one may expect an increase in net magnetic moment ($n_{net} = n_B - n_A$). With the substitution of cadmium, A-site ionic radius and lattice edges at A, B-sites have been observed to increase which leads to decrease in net A-B indirect exchange interaction and this gives rise to B-B interaction which makes B spins no longer parallel to each other[10] and so net magnetic moment decreases. This behavior has been observed by many workers in different ferrite systems [3,4,5,8] and such a variation in magnetic moment is attributed to the presence of super-magnetic clusters of paramagnetic centers [5], preparation techniques employed. A high value of saturation magnetization (104.54emu/gm) is observed for $Cd_{0.07}Co_{0.93}Fe_2O_4$ [26]. Since in the present system we observed a decrease net magnetic moment, we expect the presence of canting between spins of A and B sites and this can be estimated using the formula [27-29]

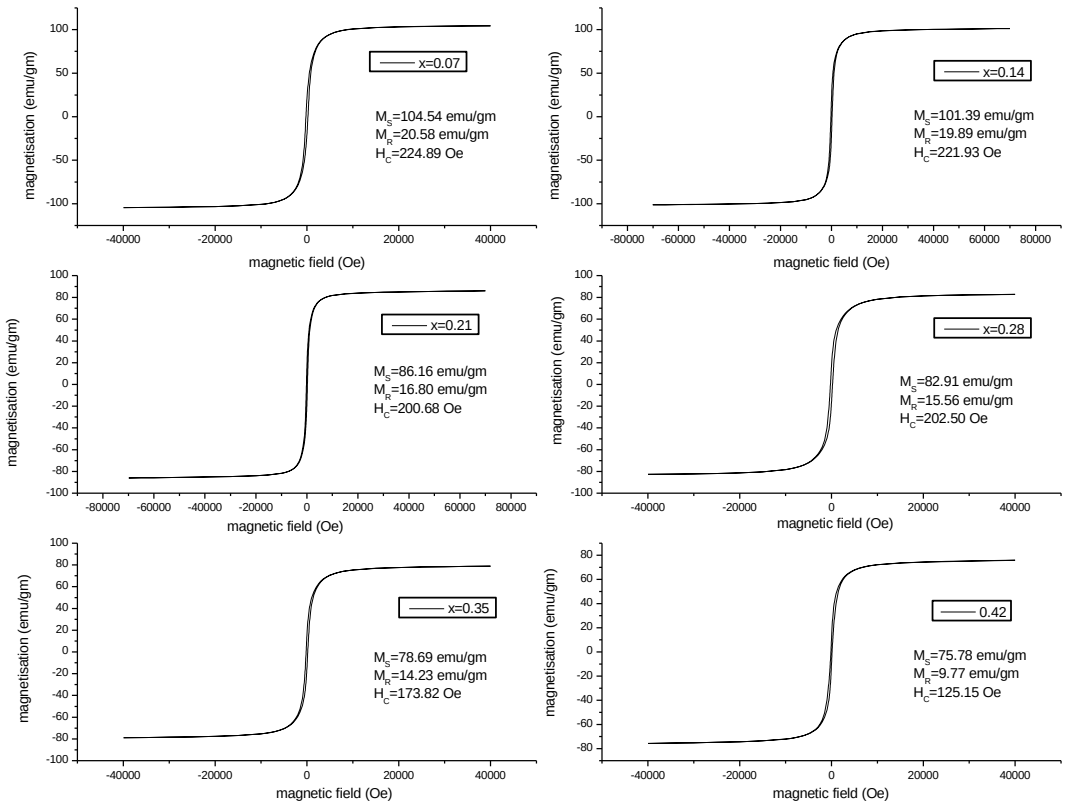

Figure 8: VSM measurements of various samples with Cd. Conc. (x).

Table 1:Variation of lattice constant, bond-length, lattice edge, υ_1, υ_2, ionic radius & force constants with increasing Cd conc.

Sample Code	Lattice Constant a(A^0)		Bond length at A-site d_{AX}(A^0)		Bond length at B-site d_{BX}(A^0)		Lattice Edge at A-site (A^0)		Lattice Edge at B-site (A^0)		Wave number (cm^{-1})		Ionic radius at B-site (A^0)		Force constant (dyne/cm)		Grain size calculated from FESEM (nm)
	exp	th	exp	th	exp	th	exp	th	exp	th	υ_1	υ_2	r_A	r_B	K_t	K_o	
X=0.07	8.408	8.408	1.820	1.820	2.102	2.102	3.641	3.641	2.973	2.973	585	395	0.683	0.677	2.508	1.143	474.05
X=0.14	8.430	8.434	1.825	1.826	2.108	2.109	3.650	3.652	2.981	2.982	583	394	0.706	0.673	2.491	1.138	540.36
X=0.21	8.455	8.460	1.831	1.832	2.114	2.115	3.661	3.663	2.989	2.991	580	394	0.729	0.670	2.465	1.138	552.86
X=0.28	8.480	8.487	1.836	1.837	2.120	2.122	3.672	3.675	2.998	3.000	579	393	0.752	0.666	2.457	1.132	463.95
X=0.35	8.510	8.513	1.843	1.843	2.128	2.128	3.685	3.686	3.009	3.010	575	393	0.776	0.663	2.423	1.132	518.52
X=0.42	8.531	8.539	1.847	1.849	2.133	2.135	3.694	3.698	3.016	3.019	573	393	0.799	0.659	2.406	1.132	436.02

Table 2—Mol.Wt, Magnetic measurement values obtained from VSM & proposed cation distribution for various samples with Cd conc.

Sample code	Proposed cation distribution for $Cd_{1-x}Co_xFe_2O_4$	Mol. Wt. of the sample (gm)	Experimental values obtained from VSM					Theoretical values obtained from proposed distribution		
			M_S (emu/gm)	M_R (emu/gm)	Hc (Oe)	M_R/M_S	$\eta_B(\mu_B)$	M_S (emu/gm)	$\eta_B(\mu_B)$	α_{YK}
X=0.07	$(Cd_{0.07}Co_{0.2}Fe_{0.73})$ $[Co_{0.73}Fe_{1.27}]$	238.37	104.54	20.58	224.89	0.197	4.46	100.52	4.29	11.39
X=0.14	$(Cd_{0.14}Co_{0.2}Fe_{0.66})$ $[Co_{0.66}Fe_{1.34}]$	242.11	101.39	19.89	221.93	0.196	4.40	110.27	4.78	17.12
X=0.21	$(Cd_{0.21}Co_{0.2}Fe_{0.59})$ $[Co_{0.59}Fe_{1.41}]$	245.85	86.16	16.80	200.68	0.195	3.79	119.72	5.27	33.64
X=0.28	$(Cd_{0.28}Co_{0.2}Fe_{0.52})$ $[Co_{0.52}Fe_{1.48}]$	249.60	82.91	15.56	202.50	0.188	3.71	128.89	5.76	39.59
X=0.35	$(Cd_{0.35}Co_{0.2}Fe_{0.45})$ $[Co_{0.45}Fe_{1.55}]$	253.34	78.69	14.23	173.82	0.181	3.57	137.78	6.25	45.14
X=0.42	$(Cd_{0.42}Co_{0.2}Fe_{0.38})$ $[Co_{0.38}Fe_{1.62}]$	257.08	75.78	9.77	125.15	0.129	3.49	146.42	6.74	49.60

The major factors which caused the decrease in magnetization with cadmium concentration in the present system are decrease in magnetic moment at A-site, increase in bond lengths and canting between spins of A and B-sites. The decrease in coercivity in the present samples has been due to decrease in cobalt content which has large magnetic anisotropy, whereas the substituting ion Cd^{2+} has zero magnetic anisotropy. The magnetic anisotropy contribution due to Fe^{3+} ions is small both at A and B-sites. The decrease in coercivity can also be attributed to increase in grain size which allows the presence of multi-domain behavior [30] and t is also confirmed by considerable decrease (table 2) in the ratio of remanence to saturation magnetization (M_R/M_S) at room temperature. The most important observation from the above table is the best agreement in experimental and calculated magnetic moments/saturation magnetization with varying cadmium content. This shows that the sol-gel method employed in the present study played an important role not only in controlling the particle size and shape but also in the variation of cation distribution at A and B-sites in the lattice. Such a distribution led to enhancement of magnetization in the present samples.

V. CONCLUSION

The present systems showed a definite hysteresis loop. The coercive force, saturation magnetization and the ratio of remanance to saturation magnetization decrease as cadmium content increases. Increase in lattice constant and dilution of A-site magnetic moment has been the main cause for the observed decrease in saturation magnetization and canted spin structure.

REFERENCES

[1] A Mahesh Kumar, M Chaitanya Varma, GSVRK Choudary, K. Srinivasa Rao, K.H. Rao, G.Gopalakrishna - Journal of optoelectronics and advanced materials, 12 (2010) 2386-2390.
[2] Shalendra Kumar, A.M.M. Farea, Khalid Mujasam Batoo, Chan Gyu Lee, B.H. Koo, Ali Yousef,Alimuddin, Physica B 403 (2008) 3604– 3607
[3] K Srinivasa Rao, A Mahesh Kumar, M Chaitanya Varma, GSVRK Choudary, KH Rao Journal of Alloys and Compounds 488, (2009) L6–L9.
[4] Y. Chen, J.E. Snyder, K.W. Dennis, R.W. McCallum, D.C.Jiles, J. Appl. Phys. 87 (2000) 5798.
[5] S. Kumar, R. Kumar, S.K. Sharma, V.R. Reddy, A. Banerjee, Alimuddin, Solid State Commun. 142 (2007) 706–709.
[6] B.Zhou, Y.W.Zhang, C.S.Liao, F.X.Cheng, C.H.Yan, L.Y.Chen, S.Y.Wang, Appl. Phys. Lett. 79(2001)1849.
[7] Shadab dabagh, Ali A Ati, S K Ghoshal, Samad Zare, R M Rosnan, Ahmed S Jbara, Zulkafli Othman, Bull.Mater.Sci.,Vol.39, No.4, August 2016, pp.1029-1037
[8] P.N. Vasambekar, C.B. Kolekar, A.S. Vaingankar, Materials Chemistry and Physics, 60, (1999) 282-285
[9] B.S. Trivedi, N.N. Jani, H.H. Joshi, R.G. Kulkarni, J. Mater. Sci. 35 (2000) 5523
[10] A.A. Ghani, A.A. Sattar, J. Pierre, J. Mag. Mag. Mater. 97 (1991) 141.
[11] A. K. Nikumbh, A. V. Nagawade, V. B. Tadke and P. P. Bakare, J. Mater. Sci. 36 (2001) 653-662.
[12] K.S.Rao, GSVRK Choudary, K.H.Rao, Ch.Sujatha Procedia Materials Science 10 (2015) 19 – 27
[13] ASTM File number 22 – 1063
[14] D. R. S. Gangaswamy, M. Chaitanya Varma, S. Bharadwaj, K. Sambasiva Rao, K. H. Rao, Journal of Superconductivity and Novel Magnetism 28(2015) 3599-3606
[15] E.Woleska, E.Riedel, W.Walski, Phys.Status Solidi(A) 132 (1992) K 51.
[16] Idem., Solid State Ionics 51 (1992) 231.
[17] Chandanarath, Anand S & Das R P, J Appl Phys, 4 (2002) 91.
[18] V.C. Mahajan, Ph. D. Thesis, Shivaji University, Kolhapur, India, 1995.
[19] M.M.Girgis and A.M.EL.Awad, Mat.Chem and Phys.36(1993) 48.
[20] V. R. Botakova, N. D. Zervey and V. P. Romanov, Phys. Status Solidi (A) **12** (1972) 623.
[21] P. Tarte and R. Collongues , *Ann. Chim. Paris.* **9** (1964) 135.

[22] R. D. Waldron , *Phys. Rev*. **99** (1955) 1727.
[23] S. Hafner , *Z. Kristallorg*. **115** (1961) 331.
[24] V.C. Mahajan, Ph. D. Thesis, Shivaji University, Kolhapur, India, 1995.
[25] C.M. Srivastava, T.T. Srinivasan, J. Appl. Phys. 53 (1982) 8184.
[26] T.R.K.Pydiraju, P.Apparao, K.Srinivasrao, M.ChaitanyaVarma and K.H.Rao, IJMTER, 4 (2017) 6.
[27] P.N. Vasambekar, C.B. Kolekar, A.S. Vaingankar, J. Mag. Mag. Mater. 186 (1998) 333.
[28] Y. YAFET and C. KITTEL , *Phys. Rev*. **87** (1952) 290.
[29] V.G.Panicker, R.V.Upadhyay, S.N.Rao, R.G.Kulkarni, J.Mater.Sci.Lett.3 (1984) 385.
[30] C. P. BEAN , *J. Appl. Phys*. **26** (1955) 1381